

Fundamental Symmetry measurements with high-Z atoms using the 2nd set of target stations at ISAC

March 17, 2008

Contents

1	Introduction	2
1.1	Structure of this report	2
2	Common concerns	3
2.1	Physics overview	3
2.2	Facility requirements and yields	3
3	The approved program	4
3.1	RadonEDM: physics motivation	4
3.1.1	RadonEDM: experimental overview	7
3.2	Anapole moments in francium: physics motivation	10
3.2.1	Anapole moments: experimental overview	12
3.2.2	Anapole moments: projected sensitivity and shift/yield requirements	13
3.3	Hyperfine anomaly	14
4	Further experiments	16
4.1	‘Forbidden’ M1 in atomic francium: physics motivation	16
4.1.1	‘Forbidden’ M1 in atomic francium: experiment	16
4.2	Atomic PNC in francium: physics motivations	17
4.2.1	Status of atomic PNC measurements	18
4.2.2	Considerations for a PNC experiment in francium	20
4.2.3	Atomic PNC in francium: experimental techniques	20
4.2.4	Signal-to-noise ratio	21
4.2.5	Neutron radius question	23
4.3	Electron EDM in francium: physics motivation	23
4.3.1	Electron EDM in francium: experimental organization and techniques . . .	23
4.4	Radon EDM using β asymmetry	24
5	Summaries	25
5.1	Beamtime summary	25
5.2	Physics summary	26

1 Introduction

This document has two main goals. One is to convince the committee that we have an ambitious and compelling program for precision measurements using radon and francium isotopes. These experiments will push state-of-the-art atomic and nuclear experimental techniques to extend TRIUMF's physics reach into the weak neutral current and time-reversal-violating sectors for the first time.

They will also eventually require enormous amounts of beamtime. No matter what yields are achieved, the relentless patience needed to hunt down and eliminate systematic errors will always require on-tap availability of the isotopes as simple to the experimenters as heating an alkali oven.

The TRIUMF neutral atom trap project, for example, is well accustomed to making reliable, turn-key collection trap technology so that efforts can go into experiments with the small amounts of ISAC beamtime available. We note that the development of this reliable front end was done with the TISOL facility, with dedicated running periods available twice a year or more. We are aware of the difficulties of determining systematic errors from precision analyses of the redundantly measured kinematic observables when followup experiments can only be scheduled bi-annually. The neutral current experiments are much more exacting and complex and could not be completed in such a mode.

Assuming the September 2008 tests on uranium oxide are successful, we will detail below how startup of these experiments could be done with finite amounts of beamtime in coexistence with the rest of the ISAC program in the existing target stations. Factors to be gained in time-sharing of the beams will be mentioned, particularly in the case of RadonEDM.

But to fully implement these experiments and achieve their enormous promise, it is clear that a dedicated target station for 500 MeV protons on actinide targets will be needed for several years. Thus the other main goal of this document is to build a compelling case to the committee for the 2nd set of target stations and for their irradiation by protons. There are other exciting experiments to be done with neutron-rich spallation products which will be documented separately, but we are convinced that this program alone justifies the new stations.

The building of the case requires lists of isotope yields. We will show a figure with yields at the start, then detail the requirements separately for each experiment, and then condense the main beamtime requirements in the summary at the end.

1.1 Structure of this report

First we will give an overview of the common physics characteristics of the programs.

For the already approved program, we will highlight the physics motivations and only sketch the experimental methods. We refer the committee to previous EEC proposals for full details. (In addition to the EEC website, we have for convenience put our EEC proposals— along with one anapole publication and the most recent full RadonEDM proposal— at trshare.triumf.ca/~trinatl/supereec. S1010's is not currently on the EEC website due to technical error.)

The approved program includes three experiments with Stage 1 approval at high priority. (E929 has in addition Stage 2 approval for shifts for xenon development work):

- S929, an electric dipole moment search in octupole-deformed radon isotopes
- S1065, an anapole moment measurement in francium isotopes
- S1010, a measurement of neutron distributions in francium via the hyperfine anomaly in

precise atomic spectroscopy.

Then we will show in varying detail other planned francium and possible radon experiments:

- a measurement of the rate of the ‘forbidden’ M1 transition between the 7S ground state and 8S excited state, which is sensitive to relativistic corrections to many-body perturbation theory
- a measurement of atomic parity violation in the 7S to 8S transition, sensitive to the strength of the weak neutral current
- a search for the electron electric dipole moment with a francium atomic fountain.
- an advanced version of radon EDM that could take advantage of much higher beam currents, avoiding the count-rate limitations of γ -ray anisotropies by using current-mode beta detection to measure the polarization precession.

All of these experiments require large amounts of beam time, and the motivation for more shifts should be clear. But we will also attempt to go beyond this obvious requirement to emphasize new possibilities opened by achieving optical density for upgraded experiments.

2 Common concerns

2.1 Physics overview

In broadest terms, these higher-Z atoms are more sensitive to possible new short-ranged interactions between leptons and quarks because the electron wavefunction overlap with the nucleus is larger. For atomic parity violation the effects scale like Z^2N with additional relativistic enhancement, and there is similar scaling for EDMs and anapole moments.

To utilize these effects, precision atomic techniques will be combined with the copious and well-controlled isotopically selected ion beams.

It should be stressed that in the LHC era, these low-energy experiments will still play a vital role. For EDMs, time reversal violation is not probed at hadron colliders. The level of time reversal seen in precision K and B physics experiments, which can be accounted for in the one CKM matrix phase, cannot explain the baryon asymmetry. Many new physics models predict EDMs at observable levels.

When new physics is discovered at the LHC, there will be difficulty knowing its couplings to the first generation. Electrons and muons can be distinguished in the detectors, but up/down quark jets cannot be distinguished from jets of other generations. Atomic parity violation and other low-energy experiments are in a unique position to answer this question. The challenge is to make them sensitive enough, which generally means part per thousand accuracy.

2.2 Facility requirements and yields

Francium and radon are spallation products and are not produced in fission. So they will require the primary 500 MeV proton beam on uranium- or thorium- based targets. Both photofission and the “two-stage” target method (proton beam producing neutron beam that then impinges on the actinide target), are excellent ways to produce clean beams of neutron-rich fission isotopes while minimizing spallation contaminants with the same mass, but they do not make any useful amount of francium or radon.

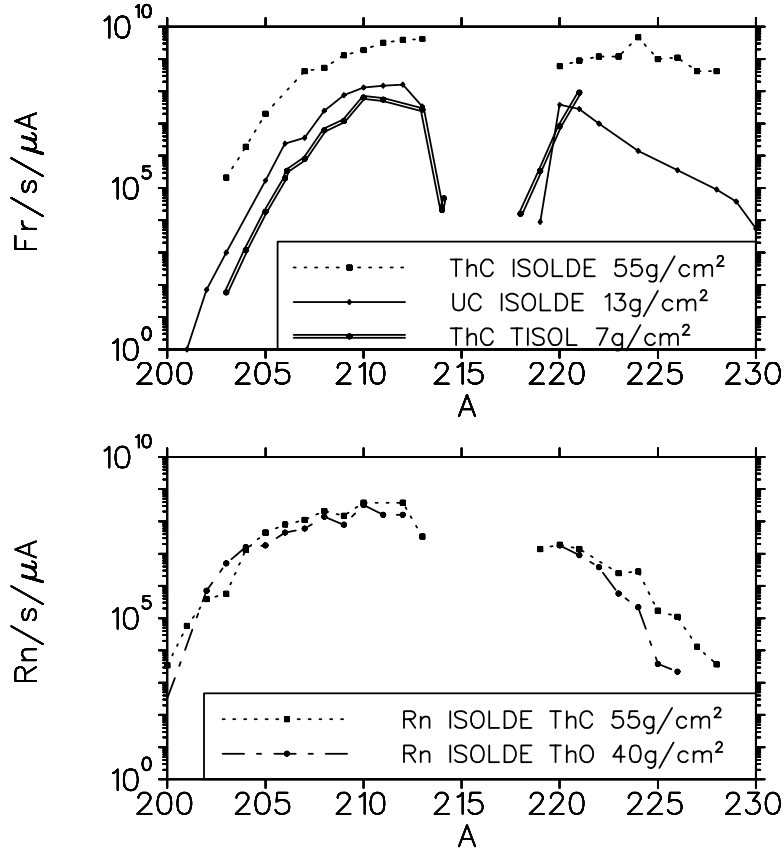


Figure 1: Yields measured at 1 μA of proton beam at ISOLDE and the TRIUMF test facility TISOL for francium and radon.

The most realistic expected result of the uranium oxide tests scheduled for September 2008 will be that we can make ISOLDE-type yields in the present target stations, i.e. approximately 1 μA of protons on relatively thick targets for weeks of running on a given target.

The most important aspect of the 2nd target stations is their potential flexibility and the possibility of a dedicated station for the actinide target. In addition, there is the possibility of much higher yields. We outline below one possibility for an upgraded radon experiment that could take advantage of qualitatively higher production.

Fig. 1 shows the experimentally measured yields of francium and radon at ISOLDE (the old 600 MeV yields most directly relevant) and at TISOL. We include them here for general reference. We will make explicit mention below within each experiment.

3 The approved program

3.1 RadonEDM: physics motivation

Studies of CP violating interactions are among the most important pursuits in modern physics with impact on the nature of elementary particle interactions and the origin of the predominance of matter over antimatter in the universe. Electric dipole moment measurements provide a unique

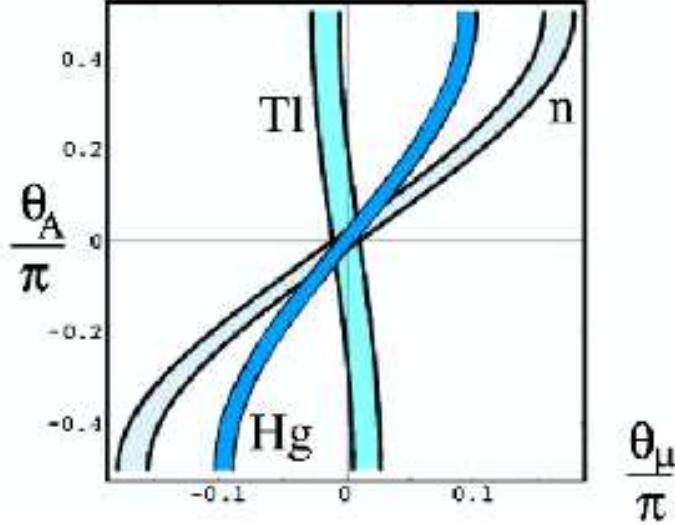


Figure 2: One explicit example of the complementarity of EDM experiments. Constraints are shown from the three types of EDM experiments: Tl (electron), Hg (J=0 atom), and neutron, on two CP-violating parameters in SUSY (Figure 8 of Ref. [17], for common superpartner mass 500 GeV and $\tan\beta=3$). The three types of EDM experiments taken together set much more powerful constraints.

and important probe of CP violation because the signal is an unambiguous violation of CP symmetry (e.g. there are no confounding final state effects), techniques of atomic and nuclear physics provide continually improving precision, and because CP violation in the K and B meson systems is dominated by Standard Model physics. The unique impact of EDMs is evident in the tight constraints on supersymmetry set by the combination of recent results from the neutron, the electron, atoms and molecules (see Fig. 2). The anticipated discovery of an EDM in one of these systems will be the first step in using CP violation to probe new physics, and measurements in several systems will, over time, fully clarify the new physics.

Measurement of the EDMs of atoms, molecules, and the neutron provide the most sensitive available probe of flavor non-changing, CP-odd physics. In the Minimal $SU(3) \times SU(2) \times U(1)$ Standard Model, CP violation enters via weak interaction flavor mixing represented by the Cabibbo-Kobayashi-Maskawa (CKM) matrix and via θ_{QCD} , the vacuum expectation value of the QCD gluon field. The CKM matrix includes a single complex phase, which successfully accounts for CP mixing in the K and B mesons. In generating an EDM, the CKM phase enters twice, with opposite sign, resulting in near cancellation and EDMs much smaller than current limits (see Fig. 3 from Ref. [1]). CP violating interactions would induce an atomic EDM (d_A) in ^{223}Rn more than 500 times larger than in ^{199}Hg . We expect to measure the atomic EDM of ^{223}Rn with precision of 10^{-26} to 10^{-27} e-cm and thus extend sensitivity to CP violation by one to two orders of magnitude.

CP violation is also a crucial component of the Sakharov mechanism of baryogenesis [2], which could explain the dominance of matter over antimatter in the Universe. In the Sakharov mechanism, the matter-antimatter asymmetry is generated in a non-equilibrium first order phase transition by CP and baryon number violating interactions; however the phase in the CKM matrix

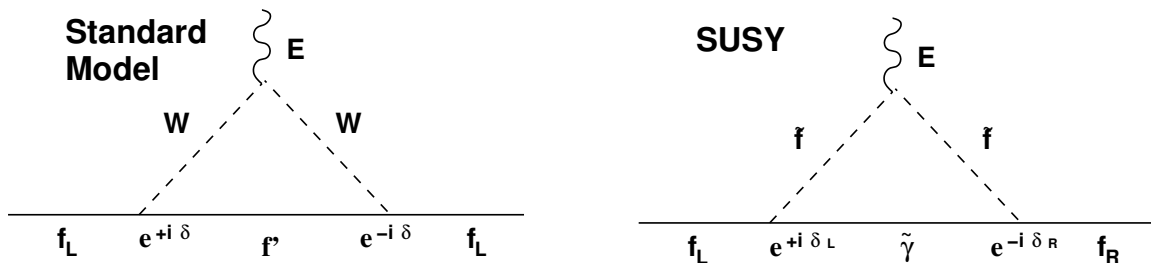


Figure 3: An example (taken from Fig. 2 of Ref. [1]) of how electric dipole moments vanish in the standard model in 1-loop order. There is only one CP-violating phase, so emission and reabsorption of a virtual W boson by a fermion (f) are time-reversals of each other, the complex number phases of the 2 processes cancel, and there is no EDM. In SUSY the phases need not be the same if, e.g., the fermion changes handedness, so EDMs are produced at this lower order.

is not sufficient to generate the observed baryon asymmetry, thus new forms of CP violation are expected [3, 4, 5]. Most significant extensions of the Standard Model introduce additional phases that could produce the baryon asymmetry and lead to EDMs many orders of magnitude larger than the CKM values [6]. For example, supersymmetric models introduce phases that could produce the baryon asymmetry at the electroweak scale and produce EDMs of atoms or the neutron close to the current limits of sensitivity [7]. In fact an electron EDM violation much smaller than the current limits could rule out electroweak baryogenesis [8], and extending the sensitivity to neutron and heavy atom EDMs would also provide strict constraints. CP violation is also a valuable observable by which to probe physics beyond the Standard Model more generally - that is, CP violation can be used to reveal a weaker interaction in the presence of the dominant strong and electroweak interactions of the Standard Model.

Radon isotopes have many attractive features for advancing sensitivity to CP violation. The most important feature is enhanced sensitivity to CP violation in isotopes with octupole deformed nuclei [9, 10, 11, 12]. For ^{223}Rn , octupole deformation leads to an enhancement of the observable atomic EDM by a factor estimated to be greater than 500 relative to ^{199}Hg [10]. Radon also provides the experimental advantages of noble gas atoms, the possibilities for multiple-species experiments that directly measure the most important systematic effects, and the promise of new techniques for precision measurement with radioactive species. The many opportunities for success of this program include the potential for discovery and precision measurement of EDMs, atomic and nuclear physics of radon isotopes, new technology, and new techniques for rare isotope physics. Ultimately, our work has the potential to achieve sensitivity to CP violation similar to or beyond that of the proposed neutron EDM experiments, which anticipate a factor of 100 improvement over the next decade [13]. The Radon-EDM Experiment also provides a co-magnetometer, which is widely considered essential for a reliable EDM measurement.

Recent theoretical advances have strengthened the case for these measurements. The work of Jon Engel and collaborators continues to clarify how octupole deformation and octupole vibrations enhance sensitivity to CP violation in the nucleus. Victor Flambaum and coworkers have reevaluated the sensitivity of the atomic EDM to CP violation in the nucleus and show that earlier calculations underestimated the sensitivity of noble gas atoms relative to ^{199}Hg . Engel and collaborators are currently calculating the enhancements in ^{223}Rn as well as several spherical isotopes

(including xenon) relevant to our program.

Measurements of atomic EDMs to date have set only upper limits on CP violating interactions. In Table 1, we show the current limits on several general mechanisms of CP violation established by experiment. CP violation generated by supersymmetry, extra Higgs bosons, or Left-Right Symmetry would generate a Schiff moment through a phenomenological quark-quark or nucleon-nucleon interaction. C_T and C_S are CP-violating tensor and scalar neutral current interactions between the atomic electrons and the nucleus. The electron and neutron EDM limits are shown to be complementary.

Table 1: Limits (90% C.L.) on phenomenological parameters of CP violation, including the most recent neutron EDM result[18] and evaluation of atomic sensitivities from reference [19]. In addition to what is shown here, the strong interaction effects are typically parameterized with additional effective meson couplings— for isoscalar and isovector parts as well as range— for which the J=0 atom and neutron experiments can be seen to be complementary.

Parameter	^{199}Hg limit[20]	Neutron limit[18]	Electron limit	Theory Ref.
θ_{QCD}	1.5×10^{-10}	4.1×10^{-10}	-	[21]
down quark EDM	-	5×10^{-26} e-cm	-	[22]
color EDM	3×10^{-26} e-cm	-	-	[21]
ϵ_q^{SUSY}	2×10^{-3}	5×10^{-3}	-	[24]
$\epsilon_q^{\text{Higgs}}$	$0.4/\tan\beta^*$	-	$0.3/\tan\beta$ (TI)[23]	[24]
x^{LR}	1×10^{-3}	5×10^{-3}	-	[24]
C_T	1×10^{-8}	-	5×10^{-7} (TIF)[26]	[25]
C_S	3×10^{-7}	-	2×10^{-7} (TI) [23]	[25]

*The ratio of masses of the two Higgs bosons in this theory is $\tan\beta$.

3.1.1 RadonEDM: experimental overview

Here we only give a very basic sketch of the experiment. For methods and a progress report we refer the committee to the December 2007 update. Publications on experimental progress can also be found in Refs. [14, 15, 16].

The RadonEDM experiment builds on existing experimental techniques with known levels of systematic error. The polarization is done through spin-exchange optical pumping with rubidium. The polarization is measured by the anisotropy of the gamma radiation, using a high-efficiency germanium array with data acquisition electronics optimized for very high count rates. See Fig. 4. Use of nuclear structure expertise is critical to find the best case, carry out the experiment, and quantify the result.

Consider an atom with angular momentum \vec{J} and electric and magnetic dipole moments d and μ . The Hamiltonian is

$$H = -(\mu\vec{B} + d\vec{E}) \cdot \vec{J}.$$

The term $\vec{E} \cdot \vec{J}$ is odd under parity and time reversal. If \vec{E} is parallel/antiparallel to \vec{B} , precession

frequency of the atom is

$$\hbar\omega = 2(\mu B \pm dE),$$

An EDM is revealed by measuring the change in precession frequency when \vec{E} is reversed with respect to \vec{B} . In the radon EDM experiment, the frequency will be measured by free induction decay.

Radon will be collected from the ISAC-1 low energy beam transport and transferred to a measurement cell using the cryogenic/gas transfer technique developed at TRIUMF and described in reference [14]. The measurement cell will contain alkali metal, preloaded and N₂ gas. The isotope ²²³Rn has a 23.2 m half-life and will be stored in the cell for about 1 hour. An EDM measurement cycle consists of polarization by laser optical pumping of the alkali-metal vapor, a $\pi/2$ pulse and free precession of the ²²³Rn in the electric (5 -10 kV/cm) and magnetic fields (1 mG). In the first EDM experiment, the free precession will be monitored by counting gamma-rays from several resolved transitions in the daughter nucleus ²²³Fr which will have an angular distribution relative to the radon \vec{J} . In Fig 4, we show the array of germanium detectors that will be used to monitor the free precession; as \vec{J} rotates, the gamma ray detection rate in each of the eight detectors will modulate at 2ω .

The precision of the frequency measurement depends on the free-precession decay time (T_2), the size of the gamma-ray anisotropy (A), the number of decays counted (N), and the background (B):

$$\sigma_d = \frac{1}{4E} \frac{1}{T_2} \frac{1}{\sqrt{\frac{1}{A^2(1-B)^2N}}}.$$

We assume $T_2 = 30$ seconds, as achieved for radon in our experiments at Stony Brook. The count rate detectable by the TIGRESS detectors will be limited to 120 kHz for the entire array, and thus we expect $\sigma_d \approx 10^{-25}$ e-cm in one day and $\sigma_d \approx 10^{-26}$ e-cm for a 100 day run of the count-rate limited experiment. With the enhanced sensitivity compared to ¹⁹⁹Hg, this would reach up to 10 times further in probing CP violation. In section 4.4, we consider free precession detection that is not count-rate limited, and the increased sensitivity that will be possible with 10 or more times greater radon production.

Senior investigators: T. Chupp, U. Michigan; Carl Svensson, P.E. Garrett, Guelph; Mike Hayden, C. Andreoiu, SFU; R.A.E. Austin, St. Mary's; Matt Pearson, Greg Hackman, Gordon Ball, John Behr, TRIUMF.

RadonEDM projected sensitivity :

The projected sensitivity for the presently planned γ -ray technique is shown in Table 2, producing a sensitivity approximately 10 times better than ¹⁹⁹Hg experiments when octupole enhancement is included. The information on "ISAC \times 20" is discussed below in Section 4.4.

The duty cycle will take the radon beam for about 1/5 the time, so the 200 shifts mentioned in the table can be shared with other experiments.

Yield estimates :

Estimates of production rates at ISAC are based on previously measured online isotope separator yields. TRIUMF's TISOL facility demonstrated 4×10^8 /sec for ²¹¹Rn and 3×10^6 /sec for ²²³Rn with 1 μ A of 500 MeV protons on a thin (6 g/cm²) uranium target. ISOLDE produced 4×10^8 /sec/ μ A

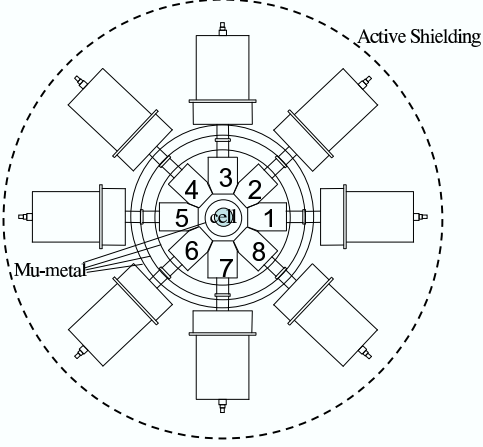


Figure 4: Schematic of the layout of eight TIGRESS detectors combined with magnetic shielding etc. for the Radon EDM experiment. Gas will be transferred to the cell.

Table 2: Count rates and statistical sensitivity for gamma-anisotropy and beta-asymmetry measurements at ISAC and ISAC \times 20 for a 100 day measurement. with $T_2 = 30$ s and $E=5$ kV/cm. The ISAC production rate for ^{223}Rn is expected to be $2 \times 10^7 \text{ s}^{-1}$.

	Gamma Anisotropy	beta asymmetry	
		ISAC	ISAC \times 20
Count Rate (s^{-1})	1.2×10^5	5×10^6	4×10^7
A	0.2	0.2	0.2
Background	0.01	0.3	0.3
Total N (100 Days)	1×10^{12}	4×10^{13}	8×10^{14}
σ_{d_A} (e-cm)	1×10^{-26}	4×10^{-27}	5×10^{-28}

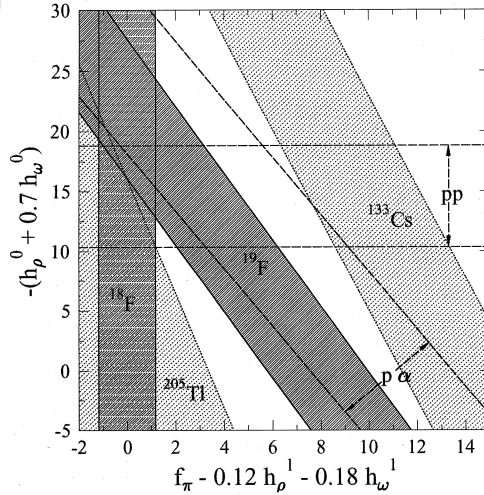


Figure 5: Constraints on isovector and isoscalar weak N-N couplings from measurement of the anapole moment of ^{133}Cs and natural thallium isotopes, compared to low-energy nuclear parity violating experiments [30].

for ^{211}Rn and $3 \times 10^6/\text{sec}/\mu\text{A}$ for ^{223}Rn with 600 MeV protons on a 55 g/cm^2 thick thorium carbide target. We expect similar production rates for ISAC with an ECR source. Conservative extrapolation suggests production rates of $2 \times 10^9/\text{sec}$ for ^{211}Rn and $2 \times 10^7/\text{sec}$ for ^{223}Rn with $10\mu\text{A}$ of 500 MeV protons at ISAC.

3.2 Anapole moments in francium: physics motivation

We present here a brief synopsis of the physics motivation. More details can be found in the S1065 proposal.

The strength of the weak neutral current in nuclear systems remains a puzzle. A member of this committee (S.F.) has noted that if the isovector weak meson-nucleon coupling f_π had been larger, weak neutral currents would have been discovered in low-energy nuclear experiments before Gargamelle's neutrino scattering. The smallness of f_π still remains a puzzle, and that value is in some conflict with the present anapole moment result (see below). It is important to clarify this issue by understanding the phenomenon better.

The anapole moment is a parity-violating electromagnetic moment produced by the weak nucleon-nucleon interaction. Quantifying it better will define both isoscalar and isovector parts of the weak nucleon-nucleon interaction in the nuclear medium. Laser trapping and cooling allows the exploitation of modern spectroscopic techniques on a small number of (radioactive) atoms.

Present measurements of the effective meson coupling constants of the weak nucleon-nucleon interaction are summarized in Fig. 5 from Ref. [30]. The measurement of the ^{133}Cs anapole moment is difficult to reconcile with low-energy nuclear parity-violating experiments. The thallium anapole moment measurement is also in some disagreement. More cases are needed to understand the basic phenomenon. (It could be said that trying to understand nuclear magnetic moments from just these same two cases would be a difficult task.)

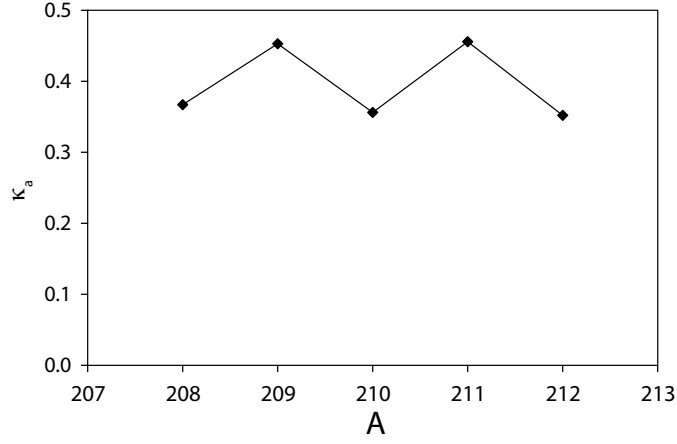


Figure 6: The anapole moment effective constant for several Fr isotopes , if polarization of the core by the valence nucleon is the main effect [27]. Then odd-even staggering will be seen as the neutrons are paired or not.

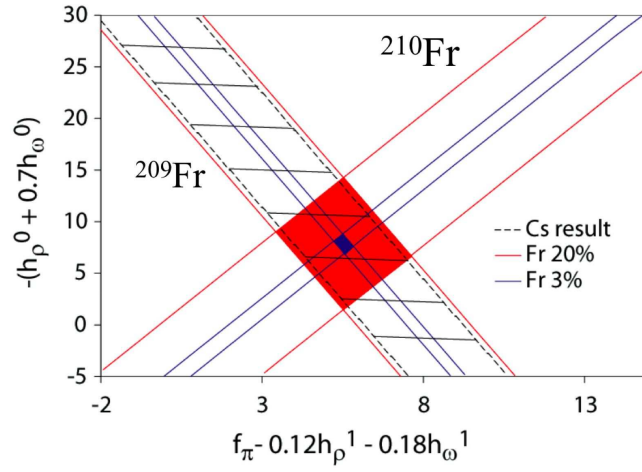


Figure 7: The anapole moments of odd-neutron and even-neutron isotopes would together constrain isovector and isoscalar weak N-N couplings. It should be noted that while the scales are the same as in Fig. 5, the band for Cs is different, because [30] used a calculation beyond the core polarization model.

The nuclear anapole comes from a number of effects, though detailed calculations suggest it is dominated by core polarization by the valence nucleons [31]. If the deliberately naive scaling shown in Fig. 6 were confirmed, that would present a direct test of this implication. Then one could extract isoscalar and isovector parts of the weak N-N interaction by comparing the odd-neutron and paired-neutron cases, as shown in Fig. 7.

If this continues to disagree with lighter nuclei and few-nucleon systems [30], this would presumably be due to the modification of the couplings in the nuclear medium [33]. The weak N-N interaction has recently been reformulated as an effective field theory, and this formalism provides a good framework in which to ask whether the effective couplings derived from few-body systems will be the same in heavier nuclei [33]. Both the γ -ray asymmetries in close-lying parity doublets in p-shell nuclei and the anapole moments in heavier nuclei then become interesting tests of this issue. The result could have implications outside of the weak N-N interaction in another problem which has been reformulated as an effective field theory: neutrinoless $\beta\beta$ decay [35]. In $0\nu\beta\beta$ there is no program of light nuclei to set the values of the coupling constants. There are four-quark effective operators that are analogous with those in the weak N-N interaction, so the degree of renormalization of the weak N-N interaction (along with information from light quark beta decay) could be an important guide to their computation. (See the last two pages of Ref. [33] for a discussion of this issue.) Since there are other phenomenological possibilities to try to account for the difficult results in close-lying parity doublets (see e.g. Appendix D of Ref. [34]), the anapole moment could become a key to this effort.

3.2.1 Anapole moments: experimental overview

An anapole experiment is currently in development. The group at Maryland is primarily responsible for the apparatus. Also contributing to that effort are the groups from William and Mary and San Luis Potosi. Details can be found in the S1065 proposal, and the physics method is described in considerable detail in Ref. [27]. We outline the technique here.

In the Boulder Cs and the Seattle Tl experiments, the anapole was extracted by determining the difference in the atomic parity violation signal on two different hyperfine transitions ($nF \rightarrow n'F'$ and $nF' \rightarrow n'F$), i.e. taking the difference of two very similar numbers. As a result, the relative error on the anapole measurement is much larger than that of the nuclear-spin independent part. One way of addressing this problem is to measure atomic parity violation on a transition where the nuclear-spin independent part is absent, e.g. within a ground state hyperfine manifold, as was proposed long ago [28, 29]. A PV-induced E1 transition between hyperfine states is driven by microwave radiation in a high-finesse cavity (see Fig. 8).

In contrast to the optical experiment, the M1 between these states is allowed and must be suppressed by orders of magnitude. Three methods can be deployed simultaneously: (i) Due to the boundary conditions in the cavity, the electric and magnetic components of the microwave field are out of phase by $\pi/2$; the atoms are collected in an optical dipole force trap which is placed in the node of the magnetic field, hence the anti-node of the electric field, resulting in a relative suppression of M1 relative to E1. (ii) An external magnetic field is aligned with respect to the microwave polarization such that M1 excitations are $\Delta m=0$ and Zeeman-detuned from the $\Delta m=1$ E1 transition which is in resonance with the microwave, yielding a further M1 suppression. In addition, for the $|4,0\rangle \rightarrow |5,-1\rangle$ transition, at a ‘magic’ magnetic field (1553 G for ^{209}Fr), the $\Delta m = -1$ E1 transition frequency is to first order independent of the magnetic field, and

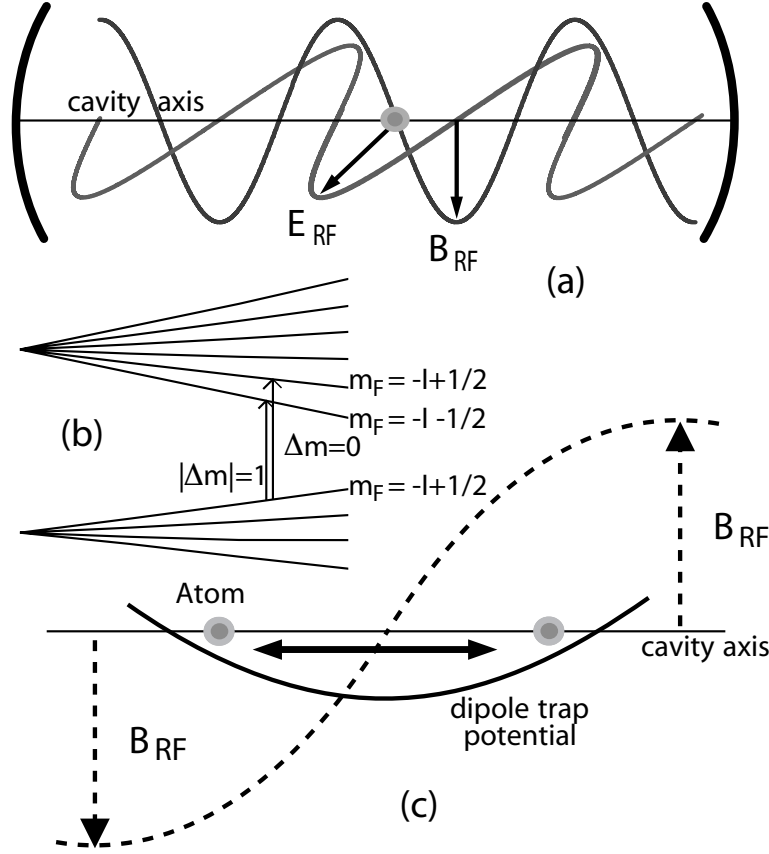


Figure 8: The suppression of the allowed M1 transition in the anapole experiment (see text for more details).

frequency noise from field fluctuations is minimized. (iii) While it is impossible to place a cloud of atoms exactly at the node of the magnetic standing wave, it is sufficient for them to oscillate symmetrically around that point, as long as the sloshing frequency is sufficiently fast compared to the duration of the microwave pulse driving the hyperfine transition. As an atom crosses the node, the phase of the magnetic field undergoes a π phase shift, and the M1-induced state evolution is reversed. Together Ref. [27] estimates that the M1 amplitude can be reduced to less than 1% of the E1 amplitude.

After irradiation with the microwaves, stimulated Raman optical transitions are then used to probe the populations of the involved states. To fulfill the conditions for a successful measurement, mainly the M1 suppression, the experiment has many exacting requirements. In particular, the correct placement of the atom cloud with respect to the standing microwave will be challenging.

3.2.2 Anapole moments: projected sensitivity and shift/yield requirements

The francium anapole moment project has four major phases: (i) francium trapping and basic spectroscopy; E1010, (ii) transfer of Fr sample into the PNC apparatus environment. (iii) observation of the PNC signal (microwave/RF or optical). (iv) isotopic chain measurements, careful study of systematic effects.

The microwave/RF anapole experiment could be started with a minimum beam flux of 10^7 Fr atoms per second, i.e. probably $<1\mu\text{A}$ on the ISAC target. Ultimately an order of magnitude more flux is highly desirable. This would enable the measurement of the anapole moments of a chain of isotopes with 10% accuracy in 250 shifts.

Phase	duration (years)	shifts (12 hrs)
(i)	2	60
(ii)	1	20
(iii)	2	100
(iv)	3	150

Table 3: Shift requirements and timeline for a microwave/RF anapole moment experiment

Senior investigators:

Gerald Gwinner, U. Manitoba, spokesman; L. Orozco, U. Maryland; S. Aubin, College of William and Mary; E. Gomez, San Luis Potosi (Mexico); Matt Pearson, John Behr, TRIUMF.

3.3 Hyperfine anomaly

Amazingly little is known about the distribution of the nuclear magnetic moment within the nucleus and, closely related, the distribution of neutrons. Electron scattering off nuclei, introduced by R. Hofstadter in the 1950s, and other effects such as isotope shifts in atomic spectra have given us quite an accurate picture of the electric charge distribution inside the nucleus. Scattering experiments probing the interaction of the electron with the nuclear magnetic moment are much harder, as the effect is small compared to the ever present electrostatic interaction. The work of A. Bohr and V. Weisskopf (Phys.Rev. 77 (1950) 94, see also H.H. Stroke *et al.*, Hyperfine Interactions 129 (2000) 319) has shown an elegant way to probe nuclear magnetism with the precise tools of atomic physics by determining the so-called hyperfine anomaly. Values for the nuclear magnetic moment are different when obtained from its interaction with an external homogeneous magnetic field on one hand, and with the field provided by an s-wave electron bound in the atom on the other, as the external field averages over the nuclear volume whereas the s-electron's radial probability density varies notably within the nuclear radius. This leads to discrepancies (of at most a few percent) in the magnetic moments determined in high fields (nuclear Zeeman splitting) and those obtained from the hyperfine splitting at low fields. Knowledge of the atomic wave function inside the nucleus in turn permits the extraction of information on the distribution of nuclear magnetism. In order to adapt this technique for use in a laser trap, the Stony Brook group developed a slight variant that operates in the low-field regime exclusively [36]. They measured and compared the hyperfine constants from the $7s$ and $7p$ states. These wavefunctions also have appreciably different overlap with the nuclear magnetic moment distribution.

Fig. 9 shows the odd-even staggering of the results from the Stony Brook work. This can be interpreted in a model which then gives information about the spatial distribution of the nuclear magnetism. This yields information about the distribution of the valence neutron in the odd-odd cases.

Extending this work to a larger range of isotopes and isomers is a natural starting point for Fr work at ISAC. The first experiments to measure the ground-state hyperfine splitting can be carried out with collinear laser spectroscopy, and the rest will require laser-cooled, trapped atoms.

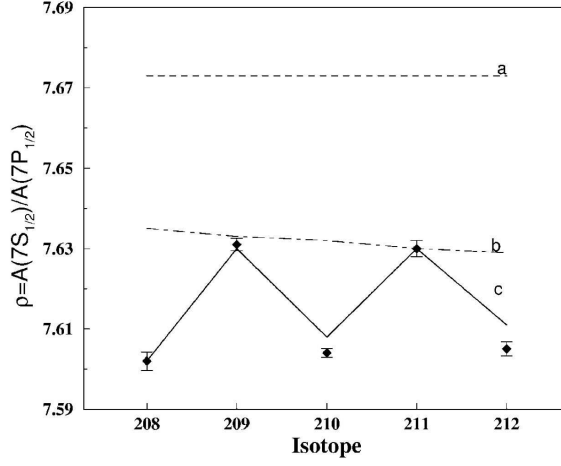


Figure 9: Hyperfine anomaly extracted from precise hyperfine splitting measurements of francium atoms [36]. The odd-even staggering shown here experimentally has similar origins to the effect expected in the anapole moment (Fig. 6). (a) point nucleus, (b) charge radius equals magnetic radius, (c) Shell model.

Details can be found in the S1010 proposal. The physics program includes detailed comparison of isomer shifts, testing the simplicity of the wavefunctions in neutron-poor spin isomers. These are very short-lived and the yields are low, so this will probably require larger beam currents and the 2nd target stations to take advantage of radiation-enhanced diffusion.

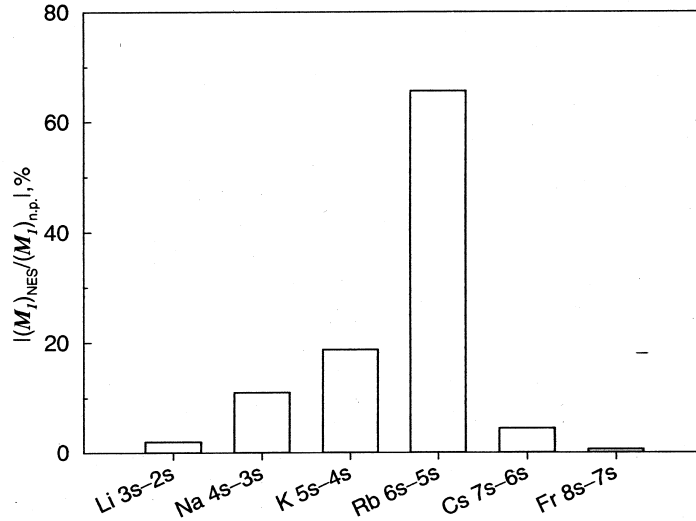


Figure 10: The ratio of the negative-energy state contribution to the no-pair contribution to the M1 strength in the alkali atoms [32].

4 Further experiments

4.1 ‘Forbidden’ M1 in atomic francium: physics motivation

The strength of the ‘forbidden’ M1 in atomic francium is sensitive to relativistic corrections to many-body perturbation theory. The percentage correction in the rubidium atom from this effect is accidentally predicted to be larger [32], as shown in Fig. 10. These effects are useful tests of the atomic theory needed to extract weak coupling coefficients from atomic parity-violation experiments.

4.1.1 ‘Forbidden’ M1 in atomic francium: experiment

A logical precursor to any optical APNC experiment in francium is the spectroscopy of the $7s \rightarrow 8s$ transition (see Fig. 11). As mentioned above, the M1 amplitude is an interesting test for atomic theory, and needs to be understood for further APNC work. Spectroscopy on this line can follow a path of increasingly difficult measurements that will help to hone the experimental skills, but starts out with a level of difficulty comparable to the spectroscopic work done at Stony Brook. Initially, the line needs to be found and observed, which is best done by driving the Stark-induced amplitude in a strong electric field (several kV/cm) in a configuration of parallel external field and laser polarization, where the large scalar transition polarizability α provides a (relatively) strong signal. Proton beam currents below $1 \mu\text{A}$ should suffice. With crossed field and polarization, the hundred times weaker transitions characterized by the vector transition polarizability β is then in reach and the ratio α/β can be determined. Observing the E1-M1 interference by flipping fields similar to the APNC procedure, produces intensity modulation at the 1 % level, about a hundred times larger than the modulation expected in APNC. This step represents a milestone. It requires

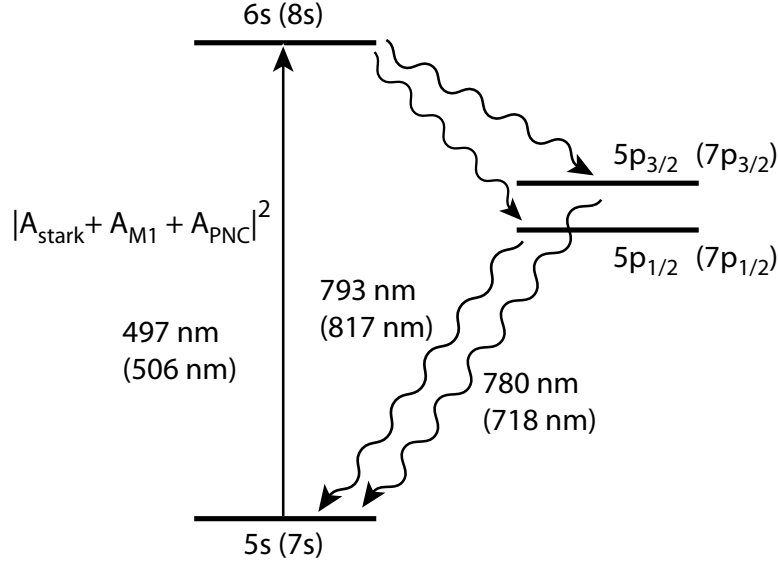


Figure 11: Most relevant atomic levels for Stark mixing experiments in rubidium and francium (with francium levels in parentheses)

the implementation of reversible, high-quality fields in the trap environment, and the quality of the signal will give crucial information about the prospects of observing a 10^{-4} modulation to better than 1 % — the eventual goal in APNC. A frequency-doubled diode-laser system capable of delivering 100 mW at 507 nm is available at Manitoba and is currently used to observe the M1 transition in rubidium at 496 nm. Incidentally, due to the near vanishing $5s \rightarrow 6s$ relativistic M1 amplitude, a Rb $\Delta F = 0$ E1-M1 interference experiment faces a comparably small intensity modulation as a Fr APNC experiment, and implementing the Rb measurement in a trap can give invaluable clues for on-line work.

A full-fledged proposal for a Fr Stark/M1 experiment will be submitted to the EEC later in 2008.

4.2 Atomic PNC in francium: physics motivations

Atomic parity violation measures the strength of the weak neutral current at very low momentum transfer.

There are three types of such “low-energy” weak neutral current measurements with complementary sensitivity. The cesium weak charge is predominantly sensitive to the neutron’s weak charge, as the proton weak charge is proportional to $1 - 4 \sin^2 \theta_W$ which accidentally is near zero. The Qweak electron scattering experiment on hydrogen is sensitive to the proton’s weak charge. The SLAC E158 Moeller scattering is sensitive to the electron’s weak charge. Different standard model extensions then contribute differently [37, 38]. E.g., the atomic parity weak charge is relatively insensitive to one-loop order corrections from all SUSY particles, so its measurement provides a benchmark for possible departures by the other “low-energy” observables. As another example, Moeller scattering is purely leptonic and so has no sensitivity to leptoquarks, so the atomic parity weak charge can then provide the sensitivity to those.

Fig. 12 shows measurements of the Weinberg angle [38]. The low-energy experiments still have

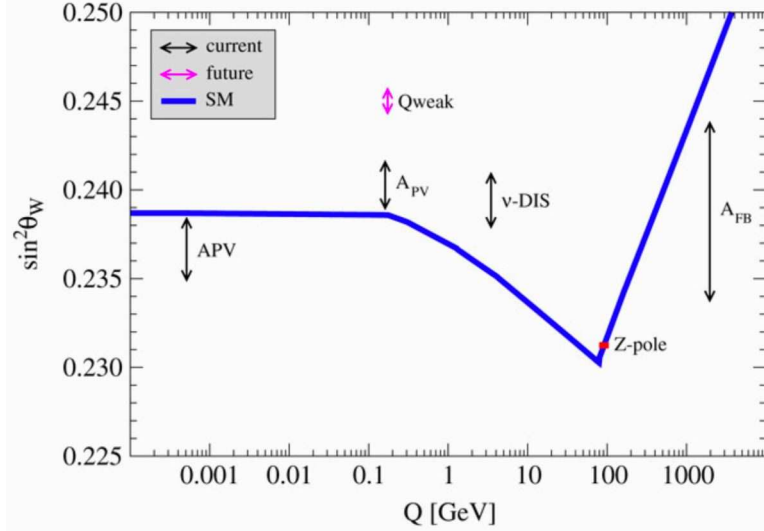


Figure 12: Measurements of the weak neutral current strength as a function of momentum transfer. Despite their lower precision, the ‘low’-energy experiments retain useful sensitivity to exchange of new bosons because they reside on the tail of the standard model Z resonance. This is Fig. 8 of Ref. [38], an update of Ref. [39].

competitive sensitivity to certain specific standard model extensions than the LEP electroweak measurements— LEP’s precision is better, but the low-energy experiments seeking terms adding to the Z exchange can have inherently more sensitivity to tree-level exchange because they work on the tail of the Z resonance. It should be stressed that Fig. 12 cannot do justice to the highly complementary nature of the low-energy experiments, as it only plots the sensitivity to one Standard Model parameter, $\sin^2 \theta_W$. Since Qweak and APNC probe different quark combinations and E158 leptons, the sensitivities to physics beyond the SM is very different. A grand unification model breaking down to E_6 symmetry adds a Z' boson on which the “low-energy” experiments still set competitive limits; in this case, the atomic parity weak charge and the Qweak experiment both have sensitivity.

Fig. 13 from Ref. [40] shows the present constraints on weak quark couplings from parity violating electron scattering and from atomic parity violation.

4.2.1 Status of atomic PNC measurements

The weak interaction in atoms induces a mixing of states of different parity, observable through PNC measurements. Transitions that were forbidden due to selection rules become allowed through the presence of the weak interaction. The transition amplitudes are generally small and an interference method is commonly used to measure them. A typical observable has the form

$$|A_{PC} + A_{PNC}|^2 = |A_{PC}|^2 + 2\text{Re}(A_{PC}A_{PNC}^*) + |A_{PNC}|^2, \quad (1)$$

where A_{PC} and A_{PNC} represent the parity conserving and parity non-conserving amplitudes. The second term on the right side corresponds to the interference term and can be isolated because it changes sign under a parity transformation. The last term is usually negligible.

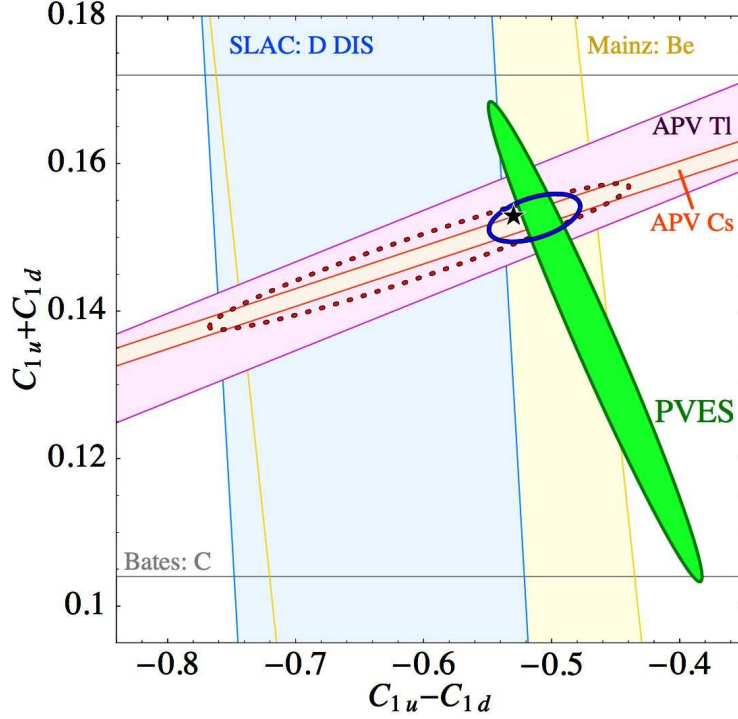


Figure 13: Constraints on weak quark couplings from electron scattering and atomic parity violation from Ref. [40], showing their complementarity.

All recent and on-going experiments in atomic PNC rely on the large heavy nucleus (large Z) enhancement factor proposed by the Bouchiat [41, 42, 43]. These experiments follow two main strategies (see recent review by M.-A. Bouchiat [44]). The first one is optical activity in an atomic vapor. The asymmetry introduced by PNC makes the atoms interact preferentially with right (or left) circularly polarized light. A linearly polarized light beam propagating through an atomic vapor experiences a rotation of the polarization plane analogous to the one observed in the Faraday effect except that in this case there is no magnetic field present. The measurement strategy uses interference with an allowed transition to enhance the small effect. The amount of rotation is related to the weak charge, which quantifies the effect of the weak force. The method has been applied to reach a precision of 2% in bismuth [45], 1.2% in lead [46, 47] and 1.2% in thallium [48].

The second strategy measures the excitation rate of a highly forbidden transition. The electric dipole transition between the $6s$ and $7s$ levels in cesium becomes allowed through the weak interaction. Interference between this transition and the one induced by the Stark effect due to the presence of an static electric field generates a signal proportional to the weak charge. The best atomic PNC measurement to date uses this method to reach a precision of 0.35% [62, 63]. The exquisite precision reached with the cesium experiment at Boulder allowed the extraction of the anapole moment from their measurement [62, 63]. The transition is dominated by the spin independent contribution, which is proportional to the weak charge. They observed a small difference in the signal depending on the hyperfine levels used for the transition. The difference corresponds to the spin dependent contribution which for cesium is dominated by the anapole moment. They

extracted the spin dependent contribution with an accuracy of 14% giving the first unambiguous measurement of an anapole moment.

Other methods have been proposed and some work is already on the way. The Bouchiat group in Paris has worked on the highly forbidden $6s$ to $7s$ electric dipole transition in a cesium cell but detects the occurrence of the transition using stimulated emission rather than fluorescence; this effort has ended after reaching 2.6% statistical accuracy [50]. The Bouchiat group has also considered more than one interesting method using laser-cooled atoms [49, 51]. The Budker group in Berkeley has been pursuing measurements in ytterbium, which has many stable isotopes available [52, 53]. There is an on-going experiment in the Fortson group in Seattle using a single barium (or alternatively radium) ion [54, 55]. The group of DeMille at Yale is planning to measure anapole moments by placing diatomic molecules in a strong magnetic field [56]. A collaboration in Russia wants to measure the anapole moment in a potassium cell [57]. The group at Legnaro and the current collaboration are working towards a PNC measurement using francium [58, 59]. This list is not intended to encompass all the efforts, but represents some of the groups interested in PNC at present.

4.2.2 Considerations for a PNC experiment in francium

In order to enhance the small parity non-conservation effect in francium, it is necessary to perform a measurement based on an ‘electroweak interference’ between a weak-interaction amplitude F_{pnc} associated with a Z^0 exchange, and a parity conserving electromagnetic amplitude F associated with photon exchanges [60]. The means of looking for such an effect consist in preparing a handed experiment, one that can be performed in either a right-handed or a left-handed configuration. One measures the transition rate in the two configurations. The results of the two experiments differ by the electroweak interference term. A right-left asymmetry

$$A_{\text{RL}} = 2 \frac{\text{Re}(F F_{\text{pnc}})}{|F|^2 + |F_{\text{pnc}}|^2} \quad (2)$$

can be defined. The electromagnetic amplitude is much larger than the weak-interaction amplitude and the experiments are designed to make the argument of the numerator real to maximize the effect, so the right-left asymmetry is simply:

$$A_{\text{RL}} = 2 \frac{F_{\text{pnc}}}{F}. \quad (3)$$

Typical numbers for the asymmetry from the cesium experiments are a few parts per million [63]. The difficulty of the experiment consists in discriminating the tiny parity violating interference against parity-conserving signals that are many orders of magnitude larger. Systematic errors come from an imperfect reversal of the handedness of the experiment and give false parity violating signals that need to be checked with the help of the redundancy in the coordinate inversions.

4.2.3 Atomic PNC in francium: experimental techniques

So far, there has been no parity non-conservation measurement in neutral atoms performed utilizing the new technologies of laser cooling and trapping. In order to create a road-map for an experiment one could assume a transition rate measurement following closely the technique used

by the Boulder group in cesium [62, 63]. We start with a Stark shift to induce a parity conserving amplitude between the $7s$ and $8s$ levels of francium and look how this electromagnetic term will interfere with the weak interaction amplitude giving rise to a left-right asymmetry with respect to the system of coordinates defined by the static electric field \mathbf{E} , static magnetic field \mathbf{B} , and the Poynting vector \mathbf{S} of the excitation field, such that the observable is proportional to $\mathbf{B} \cdot (\mathbf{S} \times \mathbf{E})$.

Francium atoms would accumulate in a magneto-optic trap (MOT). Then, after further cooling to control their velocities, they would be transferred to another region where a dipole trap will keep them ready for the measurement, which would be performed by moving the dipole trap with the atoms into the mode of a high finesse interferometer tuned to the $7s$ to $8s$ transition in a region with a DC electric field present. If an atom gets excited it will decay via the $7p$ state, but could also be ionized. Optical pumping techniques allow one to recycle the atom that has performed the parity non-conserving transition many times enhancing the probability to detect the signature photon. Redundancy in the reversal of the coordinates would suppress systematic errors. There is a strong assumption implicit in this statement that needs to be thoroughly studied: the trap does not affect the measurement.

4.2.4 Signal-to-noise ratio

To estimate the requirements for a parity non-conservation measurement in francium it is good to take the Boulder Cs experiment as a guide (see article by C. Wieman in reference [64]). The most important quantity to estimate is the signal-to-noise ratio since that will determine many of the requirements of the experiment.

The approach of Stark mixing works as an amplifier in the full sense of the word, it enlarges the signal, but it also brings noise. The Stark-induced part of the signal in photons per second is given in equation 4, this signal will contribute the shot noise to the measurement,

$$S_{\text{stark}} = \frac{16\pi^3}{3h\epsilon_o\lambda^3} E^2 \beta^2 I_o N. \quad (4)$$

The parity non-conservation signal in photons per second is

$$S_{\text{pnc}} = \frac{16\pi^3}{3h\epsilon_o\lambda^3} 2E\beta \text{Im}(E_{\text{pnc}}) I_o N, \quad (5)$$

where β is the vector Stark polarizability, E is the dc electric field used for the Stark mixing interference, N the number of atoms in the interaction volume, λ the wavelength of the transition, $\text{Im}(E_{\text{pnc}})$ is the parity non-conservation amplitude expressed as an equivalent electric field, and I_o the normalized (to atomic saturation) intensity of the excitation source. Assuming only shot noise as the dominant source of noise, the signal to noise ratio achieved in one second is:

$$\frac{S_{\text{pnc}}}{N_{\text{noise}}} = 2 \left(\frac{16\pi^3}{3h\epsilon_o\lambda^3} \right)^{1/2} \text{Im}(E_{\text{pnc}}) \sqrt{I_o N}. \quad (6)$$

For francium in the $7s$ to $8s$ state, the ratio becomes

$$\frac{S_{\text{pnc}}}{N_{\text{noise}}} = 7.9 \times 10^3 \text{Im}(E_{\text{pnc}}) \sqrt{I_o N}. \quad (7)$$

This last expression gives a result in $(\sqrt{\text{Hz}})^{-1}$ when using atomic units for the PNC term. It illustrates where a future measurement with francium is stronger: The size of the effect. The calculated value from Dzuba *et al.* [65, 66, 67] for $\text{Im}(E_{\text{pnc}})$ of 1.5×10^{-10} in atomic units is eighteen times larger than in cesium.

The ratio does not depend on the particular details of the interference experiment used; that is, the value of the vectorial Stark polarizability of the $7s \rightarrow 8s$ transition β nor the particular value of the DC electric field chosen. These factors enter in the signal-to-noise ratio once the technical noise is considered.

The very high intensities available in a standing wave will exert a repelling force that will tend to move the cold atoms to a region of low intensity. FM modulation at integers of the free spectral range of the cavity can create a slowly moving travelling envelope to solve this problem as already suggested by the Boulder group.

A serious complication for a trap-based experiment is photoionization in the excited state by the intense 507 nm radiation, which was already discussed in [61]. At intensities of 800 kW/cm² as used by Wood *et al.* [62, 63], the probability for photoionization per excitation was 10 %. In a beam experiment, where each atom is used only once, this is not particularly concerning. In a trap scenario, each atoms must be re-used over a time span of up to seconds, and hence, the photoionization rate must be brought down to a compatible level (accidentally, in Fr the situation is worse, as the 507 nm light can ionize into the continuum from both the $8s$ and the $7p_{3/2}$ states). Vieira and Wieman proposed two measures: (i) work at electric fields as low as 30 V/cm, reducing the excitation probability, but raising the fractional size of the $E_{\text{stark}}-E_{\text{pnc}}$ term; (ii) lower the intensity of the laser field. Since the M1 amplitude in Fr is about 10 times larger than in Cs (and the transition polarizabilities are comparable), electric fields below 200 V/cm do not reduce the excitation rate significantly. A reduction of the light intensity by a factor of 300 will bring the photoionization rate down to about 1 Hz. In this scenario, we have a $7s$ - $8s$ excitation rate of 30 Hz per atom. For guidance, we can refer to the Cs experiment which had a $6s - 7s$ excitation rate of 10^{10} Hz and find that 3×10^8 trapped atoms lead to the same signal, but the fluorescence modulation upon parity reversals is 2×10^{-4} , about an order of magnitude larger. The signal-to-noise with is then

$$S/N = 2 \times 10^{-4} \sqrt{30tN},$$

where t is the observation time in seconds and N the number of atoms in the trap. Or, the time to obtain a S/N with a certain excitation rate R and N atoms in the trap and an asymmetry A is

$$t = \frac{(S/N)^2}{A^2 R N}.$$

Based on these purely statistical considerations, we arrive at the following time scales:

It must be stressed that *much* more time has to be spent to deal with systematic effects. A serious concern is the E1-M1 interference that can cause a fake APNC signal. It was characterized in the Cs beam experiment making use of the atoms' motion. This option is not available in a trap setting, and a suitable alternative must be developed.

As mentioned above for the anapole moment, APNC development work can start with the expected yields in the present target stations. The new target stations would be needed for the full program.

Table 4: default

Trapped atoms	APNC measured to	time required
10^6	1.0%	2.3 hours
10^7	0.1%	23 hours
10^8	0.1%	2.3 hours

4.2.5 Neutron radius question

Since the weak charge in atoms stems mostly from the neutrons, there is some dependence on the neutron distribution in the nucleus, a quantity with few reliable experimental probes. The neutron radius measurement with parity-violating electron scattering at Jefferson Lab (‘PRex’ [68]) would result in an uncertainty on the weak charge in ^{212}Fr of 0.2% [69]. Isotopic ratios would need a next generation neutron radius experiment [69].

4.3 Electron EDM in francium: physics motivation

The physics motivation is largely shared with radon EDM, in the sense of searching for new sources of time reversal violation. Electron EDM’s have different sensitivity to the new physics sources, as we showed in Table 1 and Fig. 2.

4.3.1 Electron EDM in francium: experimental organization and techniques

A group at Lawrence Berkeley Lab has published a prototype experiment to measure the electron EDM with a cesium atomic fountain [70] including characterization of systematic errors and an outline of upgrades needed to make it competitive. Francium can be trapped in similar numbers to stable cesium, and the higher-Z atom would enhance sensitivity by more than an order of magnitude. H. Gould submitted a letter-of-intent for a francium EDM experiment at TRIUMF in the late 90’s.

A collaboration is now forming, following a ‘medium-energy’ physics plan (<http://homepage.mac.com/gould137>). There are presently 5 investigators refining potential systematic errors in various components via hardware and calculations. After it is determined what designs can work, then the apparatus can be built. It is probably a 5-year effort to make measurements in cesium. It would then be a natural extension for such a collaboration to do an experiment in francium, where an electron EDM produces an atomic EDM an order of magnitude larger [71]. Canadian university and lab collaborators would be welcomed and essential.

Electron EDM projected sensitivity Ref. [70] demonstrates techniques that may be used to improve the electron EDM sensitivity by two orders of magnitude, assuming 2×10^{14} detected atoms. An additional order of magnitude more sensitivity could then be gained by doing an experiment with the same precision using the francium atom. This can be envisioned with the high side of the projected Fr yields.

4.4 Radon EDM using β asymmetry

A possibility that could take advantage of larger yields would be current-mode beta detection.

The Radon-EDM experiment plans are to measure the free precession frequencies using γ -ray anisotropies measured with the TIGRESS or GRIFFIN detector array. The γ -ray count rate and therefore the statistical sensitivity are defined by the count-rate limit of the germanium detector array and we expect production rates of ^{223}Rn to be 5-10 times greater than the count-rate limited collection rate. One consequence is that we could run in a mode that shares the facility other experiments. More importantly, we have designed the Radon-EDM experiment with an upgrade path that will make use of any amount of ^{223}Rn produced. Designs are being considered that would put more proton beam current on the isotope production target, and yield rates of ^{223}Rn could be 10-100 times greater than the count-rate limited collection rate.

The most promising upgrade will use the **beta-asymmetry technique** that will count β 's from ^{223}Rn decay in current-mode detectors.

For the **beta asymmetry technique** we assume an analyzing power of $A = 0.2$, about half beta asymmetry for ^{223}Rn , as discussed in detail in section 4.2. The factor of two reduction is an estimate of the wash-out of the asymmetry due to multiple scattering and attenuation in 100 μm windows. This is a conservative estimate: for thinner windows, we expect sensitivity to improve linearly with the analyzing power. Backgrounds from beta-branches with small asymmetries are estimated to be 0.2. The counters will be instrumented in the current integrating mode, and the count rate will be determined by the decay rate of radon in the measurement cell, detector solid angle and efficiency. We assume the combination of solid angle and beta-efficiency of 0.5, the measured radon collection efficiency of 0.5[14], and a total count rate of 5×10^6 Hz. The resulting statistical sensitivity for the beta-asymmetry technique is 1×10^{-27} e-cm for 100 days of running at ISAC. This would extend sensitivity to CP violation by a factor of more than 100 compared to the current ^{199}Hg result. With a 20 times higher production rate at a future facility, we would expect a sensitivity of 5×10^{-28} e-cm, a sensitivity to CP violation a factor of more than 400 greater than the current neutron and ^{199}Hg results.

Beta Asymmetries: experimental details

The parity violating correlation of the momentum of emitted beta particles and the spin of the decaying nucleus is a very promising technique for Zeeman resonance detection. For beta decays, the angular correlation depends on the $\hat{J} \cdot \hat{r}$ as $R = R_0(1 + \frac{p_e}{E_e} A_\beta \hat{J} \cdot \hat{r})$. For allowed beta decays, the beta-asymmetry correlation coefficient A_β is given by

$$\xi A_\beta = \pm \kappa |g_A|^2 |<\sigma>|^2 - (g_V g_A^* + g_A g_V^*) <1> <\sigma> \sqrt{\frac{J_i}{1+J_1}}, \quad (8)$$

where the + and - correspond to β^+ and β^- decays, $\xi = |g_V|^2 |<1>|^2 + |g_A|^2 |<\sigma>|^2$, g_V and g_A are vector and axial vector couplings for the decays, and $<1>$, $<\sigma>$ are nuclear matrix elements for Fermi and Gamow-Teller transitions. The factor κ is 1, $1/(J_i + 1)$, or $-J_i/(J_i + 1)$ respectively for $J_f = J_i - 1$, J_i , $J_i + 1$. Forbidden decays are more complex, though forbidden decays would not dominate the branching ratios. For decays of radon isotopes, the beta asymmetries remain to be measured; however some estimates of A_β are possible. In Table 6 we show the beta end point energies and the correlation coefficient A_β for transitions of several radon isotopes

Table 5: Parameters used to evaluate the beta-asymmetry technique for ^{223}Rn for several branches (Branching ratios for electron capture are unknown.) The end-point energy is 1.7 MeV.

J_i^π	J_f^π	A_β	note
7/2	9/2	+7/9	100% β^- decay; pure GT
	7/2	-2/9	not pure GT
	5/2	-1	pure GT

assuming pure Gamow-Teller transitions, *i.e.* $\langle 1 \rangle = 0$. Transitions with $J_i = J_f$ are mixed, and interference may reduce A_β .

Neutron rich xenon isotopes will be used in development of the beta asymmetry technique. Beta energy discrimination is not possible, so the measurement averages the asymmetries weighted by the branching ratios. Assuming that the net asymmetry of these small branches is zero, we estimate $A_\beta \approx -0.65$. For ^{223}Rn , the β^- decays to levels in ^{223}Fr are not well known; however levels consistent with $J = 9/2$, $7/2$, and $5/2$ have been observed. We estimate an average A_β of 0.45, however the asymmetries will be measured. We plan to measure A_β for specific levels using laser optical pumping and β - γ coincidence techniques.

For an array of beta detectors similar to the azimuthal array of gamma detectors shown in Figure 5, free precession is signaled by the modulation of each detector's count rate at the Zeeman resonance frequency. The modulation in each detector is phase shifted relative to the others. The detector array would be made up of silicon detectors instrumented to count in the current integrating mode. Thin detectors would minimize sensitivity to gamma rays, the dominant background source for this technique. New EDM cells will be constructed with tapered glass side walls of thickness 100 μm or less. (This is the attenuation length for 400 keV betas; the attenuation length is roughly linear in beta energy.) In polarized electron scattering experiments E142 and E154 at SLAC[72] we used curved glass windows 80 μm thick with a differential pressure of 10 atmospheres. The curvature of the glass increases the pressure differential that can be sustained. For the EDM cells, the largest pressure differential will be about 1 atmosphere when the cell is pumped out, but a vacuum bypass may be used to eliminate any pressure differential allowing cells with very thin windows of kapton or a similar material. Windows with thickness much less than 100 μm will improve the analyzing power A .

5 Summaries

5.1 Beamtime summary

The RadonEDM experiment proposal assumed 10 μA of proton beam on a relatively thick target (see details below) for 200 shifts (100 days of beamtime) of actual counting, which would best be done in a dedicated actinide target station in the new system. Development work would be done at lower current and for shorter periods, so could commence with the present target station if the September tests are successful. A method is outlined in Section 4.4 that could take advantage of higher count rates.

The anapole moments of francium can be measured at yields of $10^8/\text{sec}$ or better, requiring about 1 μA of proton beam on thin targets for the best cases. We showed in Section 3.2.2 the S1065

proposal timeline, requiring 80 shifts of development work over 3 years that could be done in the existing stations. Actual observation of the parity-violating anapole signal is expected to take 100 shifts over 2 years, and the measurement would take 150 shifts over 3 years; these beamtimes would be best done in a dedicated actinide target station in the new stations.

Atomic PNC measurements are expected to require 10^8 /sec yields, which is still possible with $1\mu\text{A}$ of beam on a thick target for the most abundant isotopes. Anticipated timelines might be similar to the anapole experiment. Beams of $10\mu\text{A}$ would enable a greater number of isotopes to be measured to extend the neutron number reach, helping with the neutron radius phenomenology and the new physics.

The total number of “production-mode” shifts for these programs is therefore in excess of 700, not including the possibility of extra time needed for further systematic error elimination, and not including any estimate yet for a francium EDM experiment nor for a very high-current radon EDM experiment.

5.2 Physics summary

This physics program would extend TRIUMF’s long tradition in precision measurement into the neutral current sector. Searches for CP violation using EDM’s in atoms and eventually the electron would complement possible neutron EDM’s and participation in the hunt for neutrino mass matrix phases to make a comprehensive search for the source of the baryon asymmetry.

The radon experiments combine laser-driven spin exchange optical pumping with state-of-the-art gamma ray spectroscopy at extremely high count rates along with detailed nuclear structure interpretation. The francium experiments combine efficient laser trapping and cooling with extremely precise new methods.

TRIUMF currently holds several of the best experiments in the charged current sector. The success stories with the best physics reach—precision μ decay and $\pi \rightarrow e\nu$ —have had a dedicated beamline available for their entire duration.

The outlined program in precision measurement in atomic systems will require similarly exacting eliminating of systematic errors. It will be more difficult to provide the target stations needed as ISAC targets are not inherently multi-user systems, but that is the task TRIUMF must take on in order to make this program work.

References

- [1] Norval Fortson, Patrick Sandars, and Stephen Barr, ‘The Search for a Permanent Electric Dipole Moment’, *Physics Today* p. 33 June 2003.
- [2] A.D. Sahkarov, *JTEP Lett.* 5, 24 (1967).
- [3] A.D. Dolgov, (hep-ph/9707419).
- [4] M. Trodden, *Rev. Mod. Phys.* 71, 1463 (1999).
- [5] A. G. Cohen, D. B. Kaplan, and A. E. Nelson, *Ann. Rev. Nucl. Part. Sci.* **43**, 27 (1993).
- [6] M. Pospelov and A. Ritz, *Phys. Rev. D* 63, 073015 (2001).

- [7] S. Abel, S. Khalil, O. Lebedev , *Nucl. Phys.* B606, 151 (2001).
- [8] V. Cirigliano, S. Profumo, M.J. Ramsey-Musolf, hep-ph/0603246.
- [9] N. Auerbach, V.V. Flambaum, and V. Spevak, *Phys. Rev. Lett.* 76, 4316 (1996).
- [10] V. Spevak, N. Auerbach, and V.V. Flambaum, *Phys. Rev.* C56, 1357 (1997).
- [11] J. Engel, J.L. Friar, and A.C. Hayes, *Phys. Rev.* C61, 035502 (2000).
- [12] J. Engel, M. Bender, J. Dobaczewski, J.H. de Jesus, P. Olbratowski, *Phys. Rev.* C68, 025501 (2003).
- [13] R. Golub and S.K. Lamoreaux, *Phys. Rep.* 237, 1 (1994).
- [14] S.R. Nuss-Warren *et al.*, *Nucl. Inst. Meth.* **A 533**, 275 (2004).
- [15] T. Warner *et al.*, *NIM A* **538**, 135 (2005).
- [16] A.W. Phillips *et al.*, *Phys. Rev.* **C 74**, 027302 (2006).
- [17] Maxim Pospelov, Adam Ritz, ‘Electric dipole moments as probes of new physics’ *Annals of Physics* **318** 119 (2005).
- [18] C.A. Baker *et al.*, *Phys. Rev. Lett.* **97**, 131801 (2006).
- [19] V.A. Dzuba, V.V. Flambaum, J.S.M. Ginges, M.G. Koslov, *Phys. Rev.* **A 66**, 012111 (2002).
- [20] M. Romalis, W.C. Griffith, J.P. Jacobs, E.N Fortson *Phys. Rev. Lett.* 86, 2505 (2001); J.P. Jacobs, W.M. Klipstein, S.K. Lamoreaux, B.R. Heckel, and E.N. Fortson, *Phys. Rev.* A52, 3521 (1995)
- [21] M. Pospelov, and A. Ritz, *Phys. Rev. Lett.* 83, 2526 (1999).
- [22] T. Falk, K.A. Olive, M. Pospelov, and R. Roiban, *Nucl. Phys.* B560, 3 (1999).
- [23] B.C. Regan, E.D. Commins, C.J. Schmidt, D. DeMille *Phys. Rev. Lett.* 88, 071805-1 (2002).
- [24] S. Barr, *Int. J. Mod. Phys.* A8, 209 (1993).
- [25] I.B. Khripolovich and S.K. Lamoreaux. *CP Violation Without Strangeness*. Springer (1997).
- [26] D. Cho, K. Sangster, and E.A. Hinds, *Phys. Rev. Lett.* 63, 2559 (1989).
- [27] E. Gomez, S. Aubin, G.D. Sprouse, L.A. Orozco, D.P. DeMille, *Phys. Rev. A* **75** 033418 (2007).
- [28] C.E. Loving and P.G.H. Sandars, ‘On the feasibility of an atomic beam resonance experiment sensitive to the nuclear-spin-dependent weak neutral current interaction’, *J. Phys. B* **10** 2755 (1977).
- [29] E. A. Hinds and V. W. Hughes, ‘Parity nonconservation in hydrogen involving magnetic/electric resonance’ *Physics Letters B* **67** (1977) 487.

- [30] W.C. Haxton and C.E. Wieman, ‘Atomic parity nonconservation and nuclear anapole moments’, *Ann. Rev. Nucl. Part. Sci.* **51** 261 (2001).
- [31] W.C. Haxton, C.-P. Liu, and M.J. Ramsey-Musolf, ‘Nuclear anapole moments,’ *Phys. Rev. C* **65** 045502 (2002).
- [32] I.M. Savukov, A. Derevianko, H.G. Berry, and W.R. Johnson, ‘Large Contributions of Negative-Energy States to Forbidden Magnetic-Dipole Transitions Amplitudes in Alkali-Metal Atoms’, *Phys. Rev. Lett.* **83** 2914 (1999).
- [33] M.J. Ramsey-Musolf and Shelley A. Page, ‘Hadronic Parity Violation: A New View Through the Looking Glass’, *Ann. Rev. Nucl. Part. Sci.* **56** 1 (2006).
- [34] Bertrand Deplanques, ‘Parity Non-Conservation in Nuclear Forces at Low Energy: Phenomenology and Questions’ *Phys. Rep.* **297** 1 (1998).
- [35] G. Pr  zeau, M. Ramsey-Musolf, and Petr Vogel, ‘Neutrinoless double β decay and effective field theory’, *Phys. Rev. D* **68** 034016 (2003).
- [36] J.S. Grossman, L.A. Orozco, M.R. Pearson, J.E. Simsarian, G.D. Sprouse, and W.Z. Zhao, ‘Hyperfine Anomaly Measurements in Francium Isotopes and the Radial Distribution of Neutrons’, *Phys. Rev. Lett.* **83** (1999) 935.
- [37] A. Kurylov, M.J. Ramsey-Musolf, S. Su, *Phys. Rev. D* **68** 035008 (2003).
- [38] M.J. Ramsey-Musolf and S. Su, ‘Low Energy Precision Test of Supersymmetry’, *Phys. Rep.* **456** 1 (2008).
- [39] J. Erler, A. Kurylov, M.J. Ramsey-Musolf, *Phys. Rev. D* **68** 016006 (2003).
- [40] R.D. Young, R.D. Carlini, A.W. Thomas, and J. Roche, ‘Testing the Standard Model by Precision Measurement of the Weak Charges of Quarks’, *Phys. Rev. Lett.* **99** 122003 (2007).
- [41] M. A. Bouchiat and C. Bouchiat, ‘Parity Violation Induced by Weak Neutral Currents in Atomic Physics 1’, *J. Phys. (Paris)*, **35** 899 (1974)
- [42] M. A. Bouchiat and C. C. Bouchiat, ‘Weak Neutral Currents in Atomic Physics’, *Phys. Lett. B* **48** 111 (1974)
- [43] M. A. Bouchiat and C. Bouchiat, ‘Parity Violation Induced by Weak Neutral Currents in Atomic Physics 2’, *J. Phys. (Paris)* **36** 493 (1975).
- [44] M. A. Bouchiat and C. Bouchiat, ‘An atomic linear Stark shift violating P but not T arising from the electroweak nuclear anapole moment’, *Eur. Phys. J. D* **15** 5 (2001).
- [45] M.J.D. Macpherson, K.P. Zetie, R.B. Warrington, D.N. Stacey, and J.P. Hoare, ‘Precise measurement of parity nonconserving optical rotation at 876 nm in atomic bismuth’, *Phys. Rev. Lett.* **67** 2784 (1991).

- [46] D.M. Meekhof, P. Vetter, P. K. Majumder, S. K. Lamoreaux and E. N. Fortson, ‘High-precision measurement of parity nonconserving optical rotation in atomic lead’, *Phys. Rev. Lett.* **71** 3442 (1993).
- [47] D.M. Meekhof, P. Vetter, P.K. Majumder, S.K. Lamoreaux and E.N. Fortson, ‘Optical-rotation technique used for a high-precision measurement of parity nonconservation in atomic lead’, *Phys. Rev. A* **52** 1895 (1995).
- [48] P.A. Vetter, D.M. Meekhof, P.K. Majumder, S. K. Lamoreaux and E. N. Fortson, ‘Precise Test of Electroweak Theory from a New Measurement of Parity Nonconservation in Atomic Thallium’, *Phys. Rev. Lett.* **74** 2658 (1995).
- [49] S. Sanguinetti, J. Guéna, M. Lintz, Ph. Jacquier, A. Wasan, and M.-A. Bouchiat, ‘Prospects for forbidden-transition spectroscopy and parity violation measurements using a beam of cold stable or radioactive atoms, *Eur. Phys. J. D* **25** 3 (2003).
- [50] J. Guéna, M. Lintz, and M.A. Bouchiat, ‘Measurement of the parity violating 6S-7S transition amplitude in cesium achieved withing 2×10^{-13} atomic-unit accuracy by stimulated-emission detection’ *Phys. Rev. A* **71** 042108 (2005);
Jocelyne Guéna, Michael Lintz, and Marie-Anne Bouchiat, ‘Proposal for high-precision atomic-parity violation measurements by amplification of the asymmetry by stimulated emission in a transverse electric and magnetic field pump-probe experiment’, *J. Opt. Soc. Am. B* **22** 21 (2005);
J. Guéna, M. Lintz and M.-A. Bouchiat, ‘Atomic Parity Violation: Principles, Recent Results, Present Motivations’, *Modern Physics Letters A* **20** 375 (2005);
- [51] Marie-Anne Bouchiat, ‘Linear Stark Shifts to Measure the Fr Weak Nuclear Charge with Small Atom Samples’, arXiv:0711.0337v2 [physics.atom-ph]
- [52] D. DeMille, ‘Parity nonconservation in the $6s^2\ ^1S_0 \rightarrow 6s5d^3\ D_1$ transition in atomic ytterbium’, *Phys. Rev. Lett.* **74**, 4165 (1995)
- [53] J. E. Stalnaker and D. Budker and D. P. DeMille and S. J. Freedman and V. V. Yashchuk, ‘Measurement of the forbidden $6s2^1S_0 \rightarrow 5d6s^3D_1$ magnetic-dipole transition amplitude in atomic ytterbium’, *Phys. Rev. A* **66** 031403 (2002)
- [54] N. Fortson, ‘Possibility of measuring parity nonconservation with a single trapped atomic ion,’ *Phys. Rev. Lett.* **70** 2383 (1993)
- [55] T. W. Koerber and M. Schacht and W. Nagourney and E. N. Fortson, ‘Radio frequency spectroscopy with a trapped Ba^+ ion: recent progress and prospects for measuring parity violation,’ *J. Phys. B*, **36** 637 (2003)
- [56] DeMille group, retrieved April 14, 2005, from <http://pantheon.yale.edu/%7Edpd5/demilleresearch.htm>
- [57] V.F. Ezhov, M.G. Kozlov, G.B. Krygin, V.A. Ryzhov, and V.L. Ryabov, ‘On the possibility of measuring the anapole moment of potassium atom’, *Technical Physics Letters* **30** 917 (2006).

- [58] S. N. Atutov, V. Biancalana, A. Burchianti, R. Calabrese, L. Corradi, A. Dainelli, V. Guidi, B. Mai, C. Marinelli, E. Mariotti, L. Moi, E. Scansani, G. Stancari, L. Tomassetti, and S. Veronesi, ‘Trapping of Radioactive Atoms: the Legnaro Francium Magneto-Optical Trap,’ *Physica Scripta*, T105 15 (2003)
- [59] L. A. Orozco in ‘Trapped Particles and Fundamental Physics, Les Houches 2000’, p. 125, Kluwer Academic Publishers, Amsterdam (2002), ed. S. N. Atutov and R. Calabrese and L. Moi,
- [60] I. B. Khriplovich, ‘Parity Non-Conservation in Atomic Phenomena’, Gordon and Breach, New York, (1991)
- [61] D. J. Vieira and C. E. Wieman. ‘Parity nonconservation measurements of trapped radioactive isotopes - a precise test of the standard model,’ Technical report, Los Alamos, 1992.
- [62] C.S. Wood, S.C. Bennett, D. Cho, B. Masterson, J.L. Roberts, C.E. Tanner, and C.E. Wieman, ‘Measurement of parity nonconservation and an anapole moment in cesium’, *Science* **275** 1759 (1997).
- [63] C.S. Wood, S.C. Bennett, J.L. Roberts, D. Cho, and C.E. Wieman, ‘Precision measurement of parity nonconservation in cesium’, *Can. J. Phys.* **77** 7 (1999).
- [64] P. Langacker, editor. *Precision Tests of the Standard Electroweak Model*, World Scientific, Singapore, 1995.
- [65] M.S. Safronova and W.R. Johnson, ‘High-precision calculation of the parity-nonconserving amplitude in francium,’ *Phys. Rev. A* **62** 022112 (2000).
- [66] V.A. Dzuba, V.V. Flambaum, and M.S. Safronova, ‘Breit interaction and parity nonconservation in many-electron atoms’, *Phys. Rev. A* **73** 022112 (2006).
- [67] V.A. Dzuba, V.V. Flambaum, and O.P. Sushkov, ‘Calculation of energy levels, E1 transition amplitudes, and parity violation in francium,’ *Phys. Rev. A* **51** 3454 (1995).
- [68] C.J. Horowitz, S.J. Pollock, P.A. Souder, and R. Michaels, ‘Parity violating measurements of neutron densities’, *Phys. Rev. C* **63** 025501 (2001); Jefferson Laboratory Experiment E-00-003, Spokespersons R. Michaels, P.A. Souder, G.M. Urciuoli.
- [69] Tapas Sil, M. Centelles, X. Viñas, and J. Piekarewicz, ‘Atomic parity nonconservation, neutron radii, and effective field theories of nuclei’, *Phys. Rev. C* **71** 045502 (2005).
- [70] Jason M. Amini, Charles T. Munger, Jr., and Harvey Gould, ‘Electron electric-dipole-moment experiment using electric-field quantized slow cesium atoms’, *Phys. Rev. A* **75** 063416 (2007).
- [71] T. M. Byrnes, V. A. Dzuba, V. V. Flambaum, and D. W. Murray, ‘Enhancement factor for the electron electric dipole moment in francium and gold atoms’, *Phys. Rev. A* **59**, 3082 (1999).
- [72] J.R. Johnson *et al.*, *Nucl. Inst. Meth. A* 356, 148 (1995).